WARWICK
THE UNIVERSITY OF WARWICK

Original citation:
Zhang, Junliang, Gody, Guillaume, Hartlieb, Matthias, Catrouillet, Sylvain, Moffat, J. and Perrier, Sébastien. (2016) Synthesis of sequence-controlled multi-block single chain nanoparticles by a step-wise folding-chain extension-folding process. Macromolecules, 49 (23). pp. 8933-8942.
Permanent WRAP URL:
http://wrap.warwick.ac.uk/83939

Copyright and reuse:
The Warwick Research Archive Portal (WRAP) makes this work by researchers of the University of Warwick available open access under the following conditions. Copyright © and all moral rights to the version of the paper presented here belong to the individual author(s) and/or other copyright owners. To the extent reasonable and practicable the material made available in WRAP has been checked for eligibility before being made available.

Copies of full items can be used for personal research or study, educational, or not-for profit purposes without prior permission or charge. Provided that the authors, title and full bibliographic details are credited, a hyperlink and/or URL is given for the original metadata page and the content is not changed in any way.

Publisher's statement:
"This document is the Accepted Manuscript version of a Published Work that appeared in final form in Macromolecules copyright © American Chemical Society after peer review and technical editing by the publisher.
To access the final edited and published work
http://pubs.acs.org/page/policy/articlesonrequest/index.html ."

A note on versions:
The version presented here may differ from the published version or, version of record, if you wish to cite this item you are advised to consult the publisher's version. Please see the 'permanent WRAP URL above for details on accessing the published version and note that access may require a subscription.

For more information, please contact the WRAP Team at: wrap@warwick.ac.uk

warwick.ac.uk/lib-publications

Synthesis of Sequence-Controlled Multi-block Single Chain Nanoparticles by a Step-wise Folding-Chain Extension-Folding Process

*Junliang Zhang,[1] Guillaume Gody,[1] Matthias Hartlieb,[1] Sylvain Catrouillet,[1] Jonathan Moffat,[2] Sébastien Perrier[1,3,]**

[1] Department of Chemistry, The University of Warwick, Coventry CV4 7AL, UK;

[2] Asylum Research, Halifax road , High Wycombe, Buckinghamshire, HP12 3SE, UK;

[3] Faculty of Pharmacy and Pharmaceutical Sciences, Monash University, 381 Royal Parade, Parkville, Victoria 3052, Australia

*Corresponding author: Email: s.perrier@warwick.ac.uk; Tel: +44 2476 528 085

ABSTRACT

The specific activity of proteins can be traced back to their highly defined tertiary structure, which is a result of a perfectly controlled intra-chain folding process. In the herein presented work the folding of different distinct domains within a single macromolecule is demonstrated. RAFT polymerization was used to produce multi-block copolymers, which are decorated with pendant hydroxyl groups in foldable sections, separated by non-functional spacer blocks in between. OH-bearing blocks were folded using an isocyanate cross linker prior to chain extension to form single chain nanoparticles (SCNP). After addition of a spacer block and a further OH decorated block, folding was repeated to generate individual SCNP within a polymer chain. Control experiments were performed indicating the absence of inter block cross linking. SCNP were found to be condensed by a combination of covalent and supra molecu-

lar (hydrogen bonds) linkage. The approach was used to create a highly complex penta-block copolymer having three individually folded subdomains with an overall dispersity of 1.21. The successful formation of SCNP was confirmed by size exclusion chromatography (SEC), nuclear magnetic resonance (NMR), differential scanning calorimetry (DSC) and atomic force microscopy (AFM).

INTRODUCTION

The highly specialized activity of biopolymers, *e.g.* proteins, is determined by the remarkable control of their precise tertiary three-dimensional structure, which arises from the controlled folding of a single polypeptide chain.[1-5] The delicate controlled folding process of proteins is governed by the sophisticated sequence of amino-acid.[3] Reproducing the specific way in which bio-macromolecules fold their linear polymeric chains into perfectly defined nanostructures is a major, yet, challenging goal in the field of macromolecular synthesis.[5-7] Inspired by this model of biopolymers, folding a single linear polymer chain into a single chain nanoparticle (SCNP) has been recognized as a robust strategy for the construction of biopolymeric nanoparticles with potential applications in catalysis, sensing or biotechnology.[8-14] Although the design and synthesis of single chain objects has recently received great attention,[15] the development in this field is still in its initial phase. So far, several types of strategies to mediate the single chain collapse to form SCNPs have been explored,[16-22] ranging from hydrogen bonding,[23-27, 10, 28-31] covalent bonding,[32-36] to dynamic covalent bonding.[37-40] All these recent advances have provided versatile approaches to induce the folding of a single polymer chain. However, the limitation of most of these approaches is the lack of control regarding the polymer sequence and, therefore, lacking precision of the foldable moieties. The controlled folding process, however, is inarguably crucial for the specified functions of the proteins as the incorrect folding of proteins is the origin of a wide variety of pathological conditions and cause of prevalent diseases.[3] In order to mimic the incredible precision of the controlled folding process of biopolymers, controlling the sequence of the polymer chain becomes the first significant issue to address. Multi-block polymers have, therefore, attracted considerable attentions since the

sequences of the multi-block polymers can be controlled on demand. During the last few years, great developments in well-defined multi-block copolymers have been achieved using RAFT, ATRP or NMP.[41-43, 1, 44-46] These polymerization methods enable the synthesis of tailored polymeric chains with well-controlled sequences. By introducing foldable functionalities in a defined region of a single polymer chain, the folding of a specific sequence can then be controlled on demand.

All of the above results have paved the way for synthesizing more elaborated SCNPs to approach the aim of mimicking nature. Recently, Lutz *et al.* reported the intramolecular double compaction of sequence-controlled linear macromolecules into structured random coils at dilute concentrations.[47] This strategy makes a wide variety of tailored polymeric single-chain microstructures attainable and provides new perspective to build complex SCNPs. So far, the investigation about preparing more than two compacted subdomains in one single sequence controlled polymer chain by a repeated "folding-chain extension-folding" process has not been reported.

Herein, we report the synthesis of multi-block "pearl necklace" shape SCNPs by stepwise "folding-chain extension-folding" of sequence-coded block copolymers. As shown in **Scheme 1**, the first step was to synthesize a linear copolymer by RAFT polymerization. In this copolymer, OH-functionalities were introduced as foldable units being able to be cross linked using a bi-functional molecule.

Scheme 1. *Schematic Representation of the Synthesis of the Multi-block Single Chain Nanoparticles by a Repeated Folding-Chain Extension-Folding Process.*

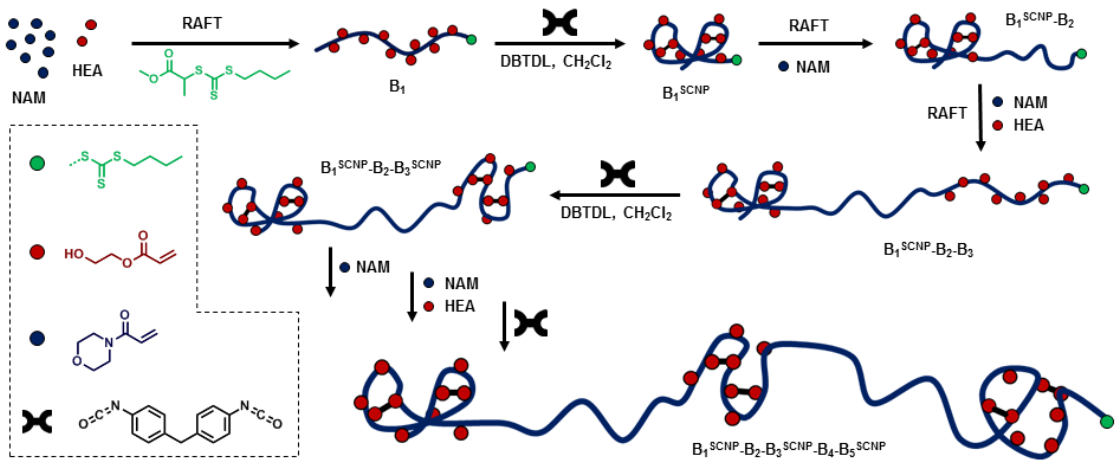

In order to satisfy the demands of the continuous addition method and prevent inter-molecular cross linking, the reaction between the cross linker and the foldable units must proceed rapid.[48] Isocyanates were chosen as they rapidly and quantitatively react with a wide range of nucleophiles (such as amines, thiols, alcohols, and carboxylic acids) under mild reaction conditions, without the production of a by-product.[49] After folding of the first block, a spacer was introduced by chain extension with a non-functional monomer, followed by the introduction of a second foldable block, which again was folded using isocyanates. This procedure was repeated one more time to yield a penta-block consisting of three individual SCNPs each separated by a polymeric spacer representing a molecular pearl necklace.

MATERIALS AND METHODS

Materials.

Milli-Q water was used as the solvent for polymerizations. 1, 4-Dioxane was obtained from Fisher Scientific and used as received. Silica gel for column chromatography was Merck Kieselgel 60 (230-400 mesh, ASTM). 4-acryloylmorpholine (NAM, Sigma-Aldrich, 97%) was filtered through a basic aluminium oxide (activated, basic, BrockmannI, standard grade, B150 mesh, 58Å) column before use to remove the radical inhibitor. 2-Hydroxyethyl acrylate (HEA, 96%) was obtained from Sigma Aldrich. HEA was purified following a previously reported protocol.[50] 2, 2′-azobis[2-(2-imidazolin-2-yl)propane]dihydrochloride (VA-044, Wako) was used without further purification. Dimethyl 2, 2’-

azobis(2-methylpropionate) (V601) was used without further purification. All polymerizations were carried out under a nitrogen atmosphere. 4, 4′-Methylenebis(phenyl isocyanate) (MDI, 98%) and *p*-Tolyl isocyanate was obtained from Sigma Aldrich and used as received. Diethyl ether (99.8%), anhydrous DCM (99.8%), methanol (99.6%), 1-(3-Dimethylaminopropyl)-3-ethylcarbodiimide hydrochloride (EDC x HCL, 98%), 4-dimethylaminopyridine (DMAP, 99%) and dibutyltin dilaurate (DBTDL, 95%) were obtained from Sigma Aldrich and used as received. Chloroform-*d* ($CDCl_3$, 99.8% D atom) and dimethyl sulfoxide-d6 (DMSO-d_6, 99.9% D atom) obtained from Sigma Aldrich were used for ^{1}H NMR analysis. 2-(((butylthio)-carbonothioyl)thio)propanoic acid (called (propanoic acid)yl butyl trithiocarbonate (PABTC) in this paper) was prepared according to a previously reported procedure.[51]

Methods.

Nuclear Magnetic Resonance (NMR) spectroscopy (^{1}H NMR and ^{13}C NMR). Spectra were recorded on a Bruker Avance III HD 400 spectrometer (400 MHz for proton and 100MHz for carbon) or a Bruker Avance III 600 (600 MHz for proton) at 27 °C in deuterated chloroform ($CDCl_3$) or deuterated DMSO (DMSO-d_6). Chemical shift values (δ) are reported in ppm. The residual proton signal of the solvent (δ_H = 7.26 ppm in $CDCl_3$, δ_H = 2.51 ppm in DMSO-d_6) was used as internal reference. For ^{13}C NMR, the carbon signal of the solvent (δ_C = 77.03 ppm in $CDCl_3$) was used as internal reference.

Determination of monomer conversions. The conversions of the monomers were determined by comparing the integration of the vinyl protons (δ ~ 6.50–5.50 ppm) to the integration of the three methyl protons belonging to the Z group of the MPABTC chain transfer agent (–CH_2–CH_3) or by comparing the integration of the vinyl protons (δ ~ 6.50–5.50 ppm) before and after reaction using mesitylene as external reference.

Size Exclusion Chromatography (SEC). Number-average molar masses ($M_{n,SEC}$) and dispersity values ($Đ$) were determined using size exclusion chromatography with either $CHCl_3$ or DMF as an eluent. The $CHCl_3$ Agilent 390-LC MDS instrument was equipped with differential refractive index (DRI), and two wavelength UV detectors. The system was equipped with 2 x PLgel Mixed D columns (300 x 7.5 mm)

and a PLgel 5 μm guard column. The eluent is $CHCl_3$ with 2 % TEA (triethylamine) additive. Samples were run at 1 mL min^{-1} at 30 °C. Poly(methyl methacrylate), and polystyrene standards (Agilent Easy Vials) were used for calibration. H_2O or Ethanol was used as a flow rate marker. Analyte samples were filtered through a PVDF membrane with 0.22 μm pore size before injection. Respectively, experimental molar mass ($M_{n,SEC}$) and dispersity ($Đ$) values of synthesized polymers were determined by conventional calibration using Agilent GPC/SEC software. The DMF Agilent 390-LC MDS instrument equipped with differential refractive index (DRI), viscometry (VS), dual angle light scatter (LS) and dual wavelength UV detectors. The system was equipped with 2 x PLgel Mixed D columns (300 x 7.5 mm) and a PLgel 5 μm guard column. The eluent is DMF with 5 mmol NH_4BF_4 additive. Samples were run at 1 mL min at 50 °C. Poly(methyl methacrylate) standards (Agilent EasyVials) were used for calibration. Analyte samples were filtered through a nylon membrane with 0.22 μm pore size before injection. Respectively, experimental molar mass ($M_{n,SEC}$) and dispersity ($Đ$) values of synthesized polymers were determined by conventional calibration using Agilent GPC/SEC software.

Differential Scanning Calorimetry (DSC). The experiments were performed to determine the thermal behavior of the synthesized polymers on a Mettler Toledo DSC1. In all tests, a scan rate of 10 K/min was used in the temperature range of -30 to 180 °C for three heating and cooling cycles. The T_g value is the maxima of the first derivative of (dH/dT).

Dynamic Light Scattering (DLS). The DLS measurements were performed on a MALVERN Instrument operating at 25 °C with a 633-nm laser module. Measurements were made at a detection angle of 173° (back scattering). The polymer solutions were prepared by dissolving the polymer samples in chloroform (1 mg/mL), which were filtered through a PVDF membrane with 0.22 μm pore size before being analysed.

Atomic Force Microscopy (AFM). AFM images were acquired in AC mode on a Cypher S system (Oxford Instruments Asylum Research). The probes used were the AC160TS from Olympus probes with a nominal resonant frequency of 300 kHz and a spring constant of approximately 40 N m^{-1} on a Multi-

mode AFM (Oxford Instruments Asylum Research). Images were acquired over a scan size of 1 μm at a pixel resolution of 512 and a scan rate of 1 Hz. Samples were diluted to 1 μg mL^{-1} in chloroform or dichloromethane and 10 μL of solution was drop-deposited onto freshly cleaved mica discs. The data were analyzed by the Asylum Research software.

RAFT polymerization. CTA, monomer and azoinitiator were charged into a flask having a magnetic stirring bar. The flask was sealed with a rubber septum and degassed with nitrogen for 15 min. The solution was then allowed to stir at the desired temperature in a thermos-stated oil bath for the desired time. After reaction, the mixture is cooled down in cold water to room temperature and open under air. A sample is taken for ^{1}H NMR (to determine monomer conversion) and SEC analysis (to determine $M_{n.SEC}$ and $Đ$). See the supporting information for detailed procedure.

Single chain nanoparticles (SCNP) synthesis. The copolymer precursor was dissolved in dry DCM ($[OH]_0$= 0.01 M). MDI (0.5 eq. of n(-OH)) was dissolved in dry DCM (the volume of the solution of MDI was kept the same with the volume of the solution of the polymer). DBTDL was added to the solution of MDI as catalyst. Both the solution of copolymer precursor and MDI were degassed by N_2 for 5 min. Subsequently, the solution of the copolymer precursor was added to the solution of MDI (with vigorous stirring) at 2 mL h^{-1} using a syringe pump at room temperature. After addition of the solution of the copolymer precursor, the reaction mixture was left for 2 h to let the reaction to complete. Then excess amount of methanol was added to the reaction mixture to quench unreacted MDI. Subsequently, the reaction mixture was evaporated to dryness under reduced pressure. Then the crude product was dissolved in minimum amount of DCM and precipitated in diethyl ether. See the supporting information for detailed procedure.

RESULTS & DISCUSSION

In this contribution, hydroxyl groups were used as the cross linkable units. Foldable blocks were produced by copolymerizing a mixture of 2-Hydroxyethyl acrylate (HEA) and N-acryloyl morpholine

(NAM) resulting in a polymer decorated with OH functionalities. Methylene diphenyl di-isocyanate (MDI) was used as a cross linker, containing two isocyanate groups, which react rapidly with hydroxyl groups in the presence of a catalyst resulting in SCNP. Subsequently, chain extension using NAM was performed to create a spacer between individual SCNPs, followed by the addition of a further NAM/HEA block. A five block copolymer was synthesized including three blocks consisting of NAM/HEA, folded separately and separated by two NAM blocks.

Synthesis and folding of the first block (B_1 and B_1^{SCNP})

The linear polymer poly(NAM_{39}-*stat*-HEA_{10}) precursor $\mathbf{B_1}$ (first block) containing statistically distributed pendant hydroxyl units was prepared by RAFT copolymerization of NAM and HEA as depicted in **Scheme 1**. Optimized RAFT conditions, previously described for the synthesis of water soluble multiblock copolymers (Azoinitiator: VA-044 at 70 °C in H_2O)[45] were applied to provide a fast and quantitative monomer conversion while maintaining high control over molar mass, narrow dispersity and high theoretical livingness. Particular attention was paid to the use of a non-free COOH chain transfer agent (methoxy-(propanoic acid)yl butyl trithiocarbonate, MPABTC, **Scheme S1**, **Figure S1** and **S2**) to avoid any side reactions during the intramolecular cross linking step with MDI. The overall degree of polymerization of the first block was targeted to be 50 with 20% of HEA comonomer to ensure efficient intramolecular cross linking, as well as a high degree of livingness. After 2 h of polymerization, near quantitative monomer conversion (98%) was obtained from ^{1}H NMR analysis for both monomers. Size-exclusion chromatography in $CHCl_3$ revealed a mono-modal distribution and a narrow dispersity ($M_{n,th}$ = 7,000 g mol^{-1}, $M_{n,SEC}$ = 6,200 g mol^{-1}, $Đ$ = 1.12, **Figure 1** and **Table 1**). The monomer ratio and the DP were determined by ^{1}H-NMR (**Figure S3**).

As shown in **Scheme 2** the folding of the linear copolymer $\mathbf{B_1}$ was carried out by the reaction of the statistically distributed pendant cross linkable hydroxyl units using MDI in presence of the catalyst dibu-

tyltin dilaurate (DBTDL) in dry DCM (to limit degradation of the isocyanate group into a primary amine). In order to reduce the competing intermolecular cross linking of multiple chains, such reactions are usually carried out at high dilutions (~10^{-5} – 10^{-6} mol L^{-1}).[48] However, even in dilute conditions, intermolecular cross linking is still unavoidable.[47]

Scheme 2. *A) Synthesis of the Single Chain Polymeric Nanoparticles* $\boldsymbol{B_1^{SCNP}}$ *and the Linear Control Copolymer* $\boldsymbol{B_1^{ctr}}$ *from the Precursor Copolymer* $\boldsymbol{B_1}$ *(poly(*NAM_{39}*-stat-*HEA_{10}*)).*

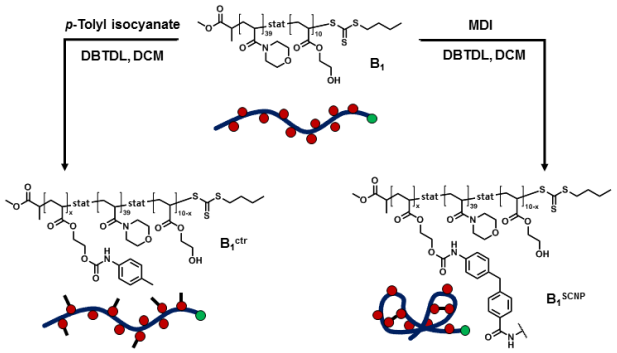

A solution to that problem was developed by Hawker *et al.* introducing a continuous addition method (by adding the solution of one reactant dropwise to the solution of the other reactant) to synthesize SCNPs.[48] This strategy also permits the synthesis of well-defined and functionalized SCNPs in a relatively high concentration (ca. 0.01 mol L^{-1}) and bigger quantities. For presented system, the slow addition of the copolymer $\mathbf{B_1}$ ([OH] = 0.01 mol L^{-1}) into a premade solution of the cross linker (MDI, 0.5 equivalent per hydroxyl group) in dry DCM was found to be the most successful approach to avoid intermolecular cross linking reactions. After 24 h remaining isocyanate groups were quenched using methanol to prevent reactions with further blocks.

In order to determine whether the single chain folding was successful and to quantify the number of reacted MDI, SEC and ^{1}H NMR studies were performed (**Table 1**). SEC is an ideal technique to monitor any changes in the hydrodynamic volume of a polymer chain allowing to distinguish between linear

precursors, intermolecular cross linked species and SCNP.[52, 4, 24, 53, 54] Comparing the SEC chromatogram of the material in chloroform after reaction ($\mathbf{B_1^{SCNP}}$) with its parent copolymer $\mathbf{B_1}$, a shift towards lower mass (*i.e.* smaller hydrodynamic volume, $M_{n,SEC}$ = 6200 g mol^{-1} to 4800 g mol^{-1}, **Figure 1**, **Figure S4**) was observed, suggesting the successful formation of single chain polymeric nanoparticles $\mathbf{B_1^{SCNP}}$. This result is consistent with previous literature about the intramolecular cross linking of a single polymer chain.[32, 48, 47, 4, 54, 35, 38, 39]

Table 1. *Characterization of the Polymers by ^{1}H NMR and $CHCl_3$-SEC.*

Sample	Composition[a]	MDI[a]	*p*TI[a]	Ureth.[a]	Urea[a]	NH_2[a]	M_n[b]	$Đ$[b]
		eq. per chain		%	%	%	g mol^{-1}	
$\mathbf{B_1}$	P(NAM$_{39}$-HEA$_{10}$)	-	-	-	-	-	6,200	1.12
$\mathbf{B_1^{SCNP}}$	P(NAM$_{39}$-HEA$_{10}$)^{SCNP}	2.4	-	44	36	20	4,800	1.27
$\mathbf{B_1^{ctr}}$	P(NAM$_{39}$-HEA$_{10}$)^{ctr}	-	4.5	100	0	0	7,500	1.11
$\mathbf{B_1^{SCNP}}$-$\mathbf{B_2}$	P[(NAM$_{39}$-HEA$_{10}$)^{SCNP}-*b*-NAM$_{12}$]	2.4	-	44	36	20	7,000	1.19
$\mathbf{B_1^{SCNP}}$-$\mathbf{B_2}$-$\mathbf{B_3}$	P[(NAM$_{39}$-HEA$_{10}$)^{SCNP}-*b*-NAM$_{12}$-*b*-(NAM$_{29}$-HEA$_8$)]	2.4	-	44	36	20	11,100	1.15
$\mathbf{B_1^{SCNP}}$-$\mathbf{B_2}$-$\mathbf{B_3^{SCNP}}$	P[(NAM$_{39}$-HEA$_{10}$)]^{SCNP}-*b*-NAM$_{12}$-*b*-(NAM$_{29}$-HEA$_8$)^{SCNP}]	4.8	-	43	39	18	9,400	1.25
$\mathbf{B_1}$-$\mathbf{B_2}$-$\mathbf{B_3}$	P[(NAM$_{39}$-HEA$_{10}$)-*b*-NAM$_{12}$-*b*-(NAM$_{29}$-HEA$_8$)]	-	-	-	-	-	12,100	1.10
$\mathbf{(B_1}$-$\mathbf{B_2}$-$\mathbf{B_3)^{SCNP}}$	P[(NAM$_{39}$-HEA$_{10}$)-*b*-NAM$_{12}$-*b*-(NAM$_{29}$-HEA$_8$)]^{SCNP}	3.9	-	40	40	20	8,400	1.29
$\mathbf{B_1^{SCNP}}$-$\mathbf{B_2}$-$\mathbf{B_3^{SCNP}}$-$\mathbf{B_4}$	P[(NAM$_{39}$-HEA$_{10}$)^{SCNP}-*b*-NAM$_{12}$-*b*-(NAM$_{29}$-HEA$_8$)^{SCNP}-*b*-NAM$_{12}$]	4.8	-	43	39	18	10,700	1.27
$\mathbf{B_1^{SCNP}}$-$\mathbf{B_2}$-$\mathbf{B_3^{SCNP}}$-$\mathbf{B_4}$-$\mathbf{B_5}$	P[(NAM$_{39}$-HEA$_{10}$)^{SCNP}-*b*-NAM$_{12}$-*b*-(NAM$_{29}$-HEA$_8$)^{SCNP}-*b*-NAM$_{12}$-*b*-(NAM$_{41}$-HEA$_8$)]	4.8	-	43	39	18	17,500	1.20
$\mathbf{B_1^{SCNP}}$-$\mathbf{B_2}$-$\mathbf{B_3^{SCNP}}$-$\mathbf{B_4}$-$\mathbf{B_5^{SCNP}}$	P[(NAM$_{39}$-HEA$_{10}$)^{SCNP}-*b*-NAM$_{12}$-*b*-(NAM$_{29}$-HEA$_8$)^{SCNP}-*b*-NAM$_{12}$-*b*-(NAM$_{41}$-HEA$_8$)^{SCNP}]	6.5	-	57	23	20	16,000	1.21

[a] The degree of polymerization, as well as amount of cross linker were determined by ^{1}H NMR;

[b] Determined by SEC in $CHCl_3$ with PMMA used as molecular weight standards.

In order to investigate whether the observed changes in hydrodynamic volume is associated to the formation of covalent connections or hydrogen bonds between urethane units, a control copolymer $\mathbf{B_1^{ctr}}$ was synthesized by reacting the linear copolymer $\mathbf{B_1}$ with a mono-functional isocyanate (*p*-tolyl isocyanate (*p*TI), **Scheme 2**). The SEC chromatogram obtained for the polymer $\mathbf{B_1^{ctr}}$ shows a shift towards higher molar mass (**Figure 1A**, **Figure S4**). The direct comparison of the $CHCl_3$ SEC traces of $\mathbf{B_1^{SCNP}}$,

$\mathbf{B_1}$ and $\mathbf{B_1}^{\mathbf{ctr}}$ confirms that the decreased hydrodynamic volume of $\mathbf{B_1}^{\mathbf{SCNP}}$ is due to intramolecular cross linking of $\mathbf{B_1}$ to obtain a collapsed nanoparticle from a random coil. It has to be noted that all SEC measurements were conducted using a flow rate marker as internal standard to minimize the error of the measurements.

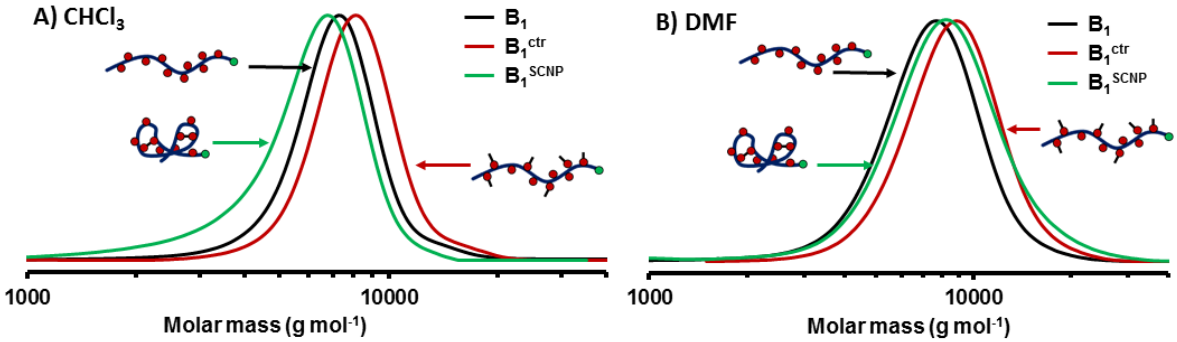

Figure 1. *SEC RI traces of* $\boldsymbol{B_1}$, $\boldsymbol{B_1}^{\boldsymbol{SCNP}}$ *and* $\boldsymbol{B_1}^{\boldsymbol{ctr}}$ *in* $CHCl_3$ *(**A**) and in DMF (**B**).*

To visualize whether the observed change in hydrodynamic volume is the result of covalent cross linking or supramolecular interactions (*e.g.* hydrogen bonds), the parent polymer, the SCNP and the control were also investigated by SEC using DMF as eluent **(Figure 1B)**. Due to its high polarity, DMF is a strong hydrogen bonding competitor solvent, which is expected to completely disrupt hydrogen bonds.[55, 56]

Surprisingly, the folded chain $\mathbf{B_1}^{\mathbf{SCNP}}$ does have an increased hydrodynamic volume in DMF compared to its parent polymer $\mathbf{B_1}$ and elutes at slightly decreased molecular weight as compared to $\mathbf{B_1}^{\mathbf{ctr}}$, which is in contradiction to the results obtained in chloroform at first sight. However, this observation could be explained by the appearance of hydrogen bonds in $CHCl_3$, which are disrupted by DMF. Indeed, covalent cross linking is not expected to be solvent sensitive. The fact that $\mathbf{B_1}^{\mathbf{ctr}}$ possesses a slightly higher hydrodynamic volume in DMF than $\mathbf{B_1}^{\mathbf{SCNP}}$, indicates that covalent cross linking is involved in the process as well. Otherwise, for a non-covalently cross linked $\mathbf{B_1}^{\mathbf{SCNP}}$ a shift of the SEC trace to higher mo-

lecular weights as compared to $\mathbf{B_1^{ctr}}$ is expected, as MDI, the cross linking agent of $\mathbf{B_1^{SCNP}}$ has a higher molar mass than *p*TI, the functionalization agent of $\mathbf{B_1^{ctr}}$. The increased R_h of B_1^{SCNP} in DMF as compared to B_1 could be a result of the increased molecular weight by the addition of multiple cross-linker molecules. As hydrogen bonds are not expected to occur in DMF, MDI is partially solubilized and contributed to an increased R_h (which contradicts the decreasing effect of R_h caused by covalent cross-linking) compared to the parent polymer.

To prove the involvement of hydrogen bonding in the cross linking process, as well as to assess the amount of reacted cross linker, ^{1}H NMR spectroscopy investigation was carried out (**Figure 2**). From the comparison of the spectra of $\mathbf{B_1^{SCNP}}$ and $\mathbf{B_1}$ in DMSO-*d6* (**Figure 2A**, **Figure S3** and **S5**) the appearance of MDI associated signals is visible (**Figure 2A**: Signal c & d). However, in addition to the signals expected for a urethane cross linked polymer, signals corresponding to urea and primary amine moieties are visible ((**Figure 2A**: Signal e & g; For a comparison with hydrolysed MDI, as well as methanol reacted MDI see **Figure S6**, **S7** and **S8**). This can be explained by the hydrophilic nature of the polymer, which leads to presence of water during cross linking reaction even though dry solvents and reagents were used. The hydrolysis of MDI leads to the presence of primary amines which, in turn, can react with isocyanate moieties to form urea units. Indeed, in the case of $\mathbf{B_1^{SCNP}}$, only 2.4 equivalents MDI per polymer chain have reacted to form urethane (44%), urea (36%) and amine groups (20%), respectively **(see Table 1)**. For $\mathbf{B_1^{ctr}}$, 4.5 equivalents of isocyanate have reacted with polymeric OH groups forming urethane bonds (**Figure S9**). The low efficiency of the reaction of MDI with the polymer in comparison to the control experiment points towards a high steric hindrance of reactive sites on the polymer after folding, which is a possible explanation for the occurrence of urea and amine groups. Once attached to the polymer chain, the remaining isocyanate cannot react with another OH-groups due to steric interaction and is hydrolysed by traces of water.

The formed amine possesses a higher reactivity towards free MDI as compared to OH groups and partially forms urea connections, which, in turn, results in an increase of hydrogen bonding in the SCNP. The presence of free primary amines further indicates the importance of steric hindrance, as the amine group has a higher tendency to react with isocyanates as compared to OH-functionalities. Indeed, the steric hindrance was not surprising and has been pointed out by Hawker *et al.*,[32] Duxbury *et al.*[57] and Berda *et al.*[53] before. Furthermore, as the cross linking reaction is carried out in dichloromethane, a solvent which does not compete with H-bonds, an additional compaction after the formation of urea and urethane functions is expected.

The presence of hydrogen bonds can also be shown by the difference between ^{1}H NMR spectra measured in DMSO-d_6 and $CDCl_3$ (**Figure 2B**). In contrast to DMSO, chloroform is not an H-bonds competitor solvent. The exchange rate of protons involved in H-bonds is drastically reduced, which leads to a broadening or a disappearance of the signals.[58] This behaviour is clearly seen on **Figure 2B**, as signals of urea have disappeared and a decrease in the integral of the urethane signals by 66% is observed.

In the case of $\mathbf{B_1^{ctr}}$, almost no change in the integral of the urethane signal could be detected proving the prevalence of covalent cross linking in the cooperative covalent and supramolecular cross linking observed for $\mathbf{B_1^{SCNP}}$. It is also likely, that the presence of urea moieties (which are known to form strong H-bonds)[59] amplifies the H-bonding potential in the cross linked polymer.

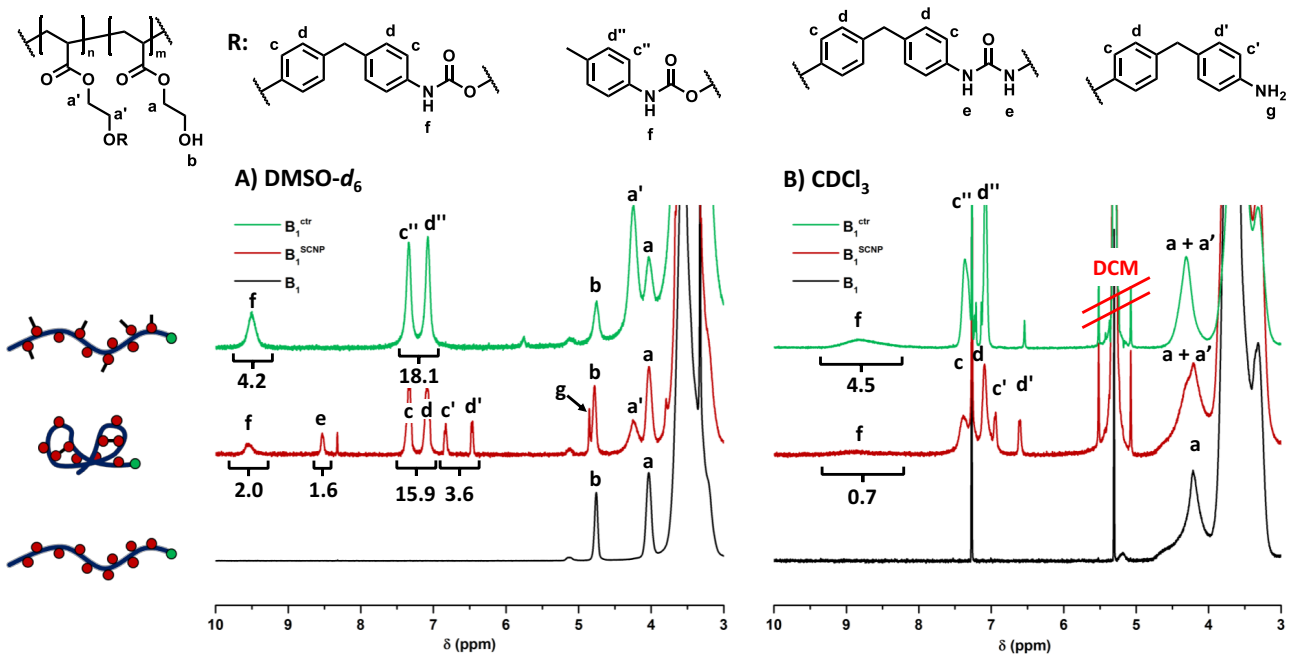

Figure 2. *^{1}H NMR spectra (400MHz) of linear polymer* $\boldsymbol{B_1}$*, folded polymer* $\boldsymbol{B_1^{SCNP}}$ *as well as control polymer* $\boldsymbol{B_1^{ctr}}$ *in DMSO- d_6 (**A**) and $CDCl_3$ (**B**), respectively.*

The successful formation of SCNPs can also be proven by differential scanning calorimetry (DSC) analysis. Due to the intramolecular cross-linking, the chain mobility will decrease compared to the linear polymer resulting in an increased glass transition temperature (T_g) value for SCNP.[48, 60, 61, 37] The T_g value of the $\mathbf{B_1^{SCNP}}$ increased significantly from the initial value of 117.2 °C for linear polymer $\mathbf{B_1}$ to 132.6 °C, while the T_g value of the $\mathbf{B_1^{ctr}}$ only increased slightly to 118.3 °C (**Figure 3**).

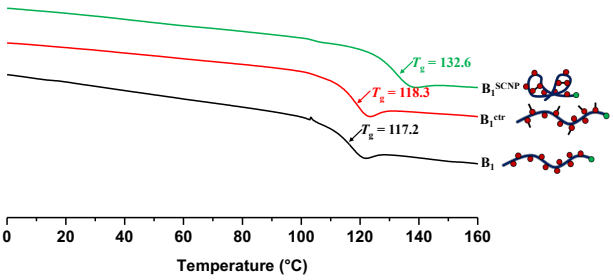

Figure 3. *DSC curves of linear polymer* $\boldsymbol{B_1}$*, control polymer* $\boldsymbol{B_1^{ctr}}$ *and folded polymer* $\boldsymbol{B_1^{SCNP}}$*.*

Dynamic light scattering (DLS) measurements in chloroform of $\mathbf{B_1}^{\mathbf{SCNP}}$ revealed a slightly bigger size ($R_h \approx 3$ nm) than the parent polymer $\mathbf{B_1}$ but a smaller R_h as compared to the control polymer B_1^{ctr} (**Figure S10** and **S11**). These results were similar to the observations of Fulton and co-workers about SCNPs.[54] They proposed possible explanations for the results. One might be a nonspherical architecture of the SCNPs, different from that of the parent linear polymer resulting in a reduced diffusion speed, thus increasing the calculated particle size. The other explanation was that the compaction of linear polymers caused the SCNPs leads to a relatively increased solubility, especially at the periphery of the particle, which contributed the increase of the volume and caused the increased values of D_h. We believe these explanations also apply to our system, especially the increase in solubility of SCNPs compared to the parent linear polymers. In our case, the cross-linker MDI attached to the polymer chains after cross-linking will highly increase the solubility of the nanoparticle material which in turn increased the value of D_h. However, the difference in size to the control polymer, which was functionalized with a smaller molecule, indicates a compaction of the SCNP.

Synthesis and folding of Triblock copolymer ($\mathbf{B_1}^{\mathbf{SCNP}}$-$\mathbf{B_2}$-$\mathbf{B_3}^{\mathbf{SCNP}}$)

As demonstrated, folding of the polymer increases steric hindrance, which will inhibit the addition of monomers to the macro-CTA. Consequently, the polymerization rate of the chain extension will be slower as compared to the polymerization of the first block at same conditions. Therefore, more initiator was required to reach full monomer conversions.

However, an increase in the propagating radical concentration will increase the termination rate and hence decrease the fraction of living chains.[62] The high livingness of the polymer chains is of paramount importance for the chain extension in order to produce multi-block copolymers. Therefore, full conversion of the monomers for the chain extensions was not targeted after the first folding process. Since $\mathbf{B_1}^{\mathbf{SCNP}}$ contains hydrophobic MDI moieties, the polymer was water insoluble. In the following chain extensions, dioxane was used as solvent. As shown in **Scheme 1**, $\mathbf{B_1}^{\mathbf{SCNP}}$ was first chain extended with a

block of poly(NAM) ($\mathbf{B_1}^{\mathbf{SCNP}}$-$\mathbf{B_2}$) at 70 °C (**Figure S12**). The DP of NAM was targeted to be 20. The monomer conversion was found to be 62% by ^{1}H NMR spectroscopy after 24 h of polymerization. Analysis of the molar mass distributions of $\mathbf{B_1}^{\mathbf{SCNP}}$-$\mathbf{B_2}$ by SEC revealed mono-modal distribution with a clear shift to higher molar mass relatively to $\mathbf{B_1}^{\mathbf{SCNP}}$ (from 4,800 g mol^{-1} to 7,000 g mol^{-1}, **Table 1**, **Figure 4**).

In order to skip purification, the polymerization mixture of $\mathbf{B_1}^{\mathbf{SCNP}}$-$\mathbf{B_2}$ was used directly for the next chain extension. The next block ($\mathbf{B_3}$) was targeted to have the same composition as the first block ($\mathbf{B_1}$). After 24 h of polymerization, the conversions of NAM and HEA, determined by ^{1}H NMR spectroscopy, were 77% and 76%, respectively. Analysis of the purified $\mathbf{B_1}^{\mathbf{SCNP}}$-$\mathbf{B_2}$-$\mathbf{B_3}$ by ^{1}H NMR spectroscopy (**Figure S13**) revealed a DP of 8 for HEA and 29 for NAM, slightly lower than expected due to the 77% of conversion of the reaction. The SEC trace of the purified $\mathbf{B_1}^{\mathbf{SCNP}}$-$\mathbf{B_2}$-$\mathbf{B_3}$ displayed mono-modal size distribution and a narrow dispersity ($M_{n,SEC}$ = 11,100, $Đ$ = 1.15, **Table 1**, **Figure 4**) with a clear shift to higher molar mass relative to $\mathbf{B_1}^{\mathbf{SCNP}}$-$\mathbf{B_2}$. The folding process of $\mathbf{B_1}^{\mathbf{SCNP}}$-$\mathbf{B_2}$-$\mathbf{B_3}$ was carried out using the same conditions used for the synthesis of $\mathbf{B_1}^{\mathbf{SCNP}}$ and was monitored by SEC and ^{1}H NMR spectroscopy analysis.

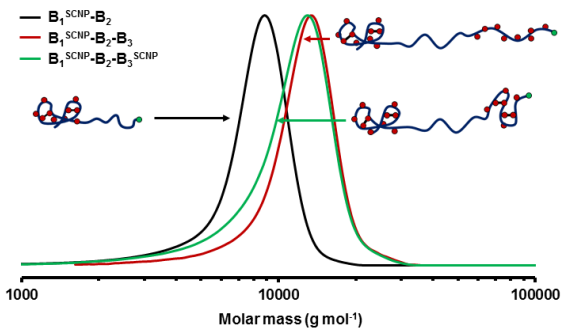

Figure 4. *SEC chromatograms (RI traces) of* $\boldsymbol{B_1}^{\boldsymbol{SCNP}}$-$\boldsymbol{B_2}$, $\boldsymbol{B_1}^{\boldsymbol{SCNP}}$-$\boldsymbol{B_2}$-$\boldsymbol{B_3}$ *and* $\boldsymbol{B_1}^{\boldsymbol{SCNP}}$-$\boldsymbol{B_2}$-$\boldsymbol{B_3}^{\boldsymbol{SCNP}}$ *in* $CHCl_3$.

As expected, the SEC trace of the polymer after cross linking reaction revealed a mono-modal chromatogram with a shift toward lower molar mass species relative to the SEC trace of the parent copolymer

of $\mathbf{B_1}^{\mathbf{SCNP}}\mathbf{-B_2-B_3}$ (from 11,100 g mol^{-1} to 9,400 g mol^{-1}, **Figure 4**, , **Figure S14, Table 1**). This result indicates that the hydrodynamic volume has decreased due to the cross linking reaction. According to the previous results on $\mathbf{B_1}^{\mathbf{SCNP}}$, this reduction in hydrodynamic volume was attributed to the intra-polymer compaction through covalent and supramolecular cross-linking. The compaction process was further analysed by ^{1}H NMR spectroscopy of the obtained products (**Figure S15**). By comparing the integrals of the MDI with the polymer backbone it was observed that (in addition to the cross linker attached to first block) 2.4 equivalents of MDI have reacted with the polymer bearing 42% of urethane units, 41% of urea units and 17% of primary amines. These values are comparable to the ratios observed for the first folding process and suggest a similar tendency to covalent and H-bond mediated cross linking. The steric hindrance after the folding of the polymer is expected to drastically reduce the reactivity of the remaining –OH of the first block of $\mathbf{B_1}^{\mathbf{SCNP}}\mathbf{-B_2-B_3}$ with the cross linker. It is, therefore, reasonable to assume that the second folding process only occurs within the third ($\mathbf{B_3}$) block.

In order to prove this assumption, a triblock linear copolymer of $\mathbf{B_1-B_2-B_3}$ (P(NAM$_{39}$-*stat*-HEA$_{10}$)-*b*-PNAM$_{12}$-*b*-(PNAM$_{29}$-*stat*-PHEA$_8$)) which has the same monomer composition as $\mathbf{B_1}^{\mathbf{SCNP}}\mathbf{-B_2-B_3}$ was synthesized (**Figures S16**, **S17** and **S18**). This triblock copolymer was then folded using standard conditions (**Scheme S2**). The folding process was studied by ^{1}H NMR spectroscopy and SEC analysis.

The ^{1}H NMR spectrum of the cross linked material of $\mathbf{(B_1-B_2-B_3)}^{\mathbf{SCNP}}$ reveals a slight decrease of the amount of attached MDI (as compared to $\mathbf{B_1}^{\mathbf{SCNP}}\mathbf{-B_2-B_3}^{\mathbf{SCNP}}$). However, a similar ratio between urethanes, urea and amines was observed (**Table 1**, **Figure S19**). Hence, a slightly decreased degree of cross linking (covalent and supra molecular) for $\mathbf{(B_1-B_2-B_3)}^{\mathbf{SCNP}}$ as compared to $\mathbf{B_1}^{\mathbf{SCNP}}\mathbf{-B_2-B_3}^{\mathbf{SCNP}}$ can be assumed.

The SEC trace of $\mathbf{(B_1-B_2-B_3)}^{\mathbf{SCNP}}$ displays a mono-modal chromatogram possessing a shift to lower molar mass compared to the linear precursor $\mathbf{B_1-B_2-B_3}$ (from 12,100 g mol^{-1} to 8,400 g mol^{-1}, **Figure 5**, **Figure S20, Table 1**). Most importantly, the shift in hydrodynamic volume is more pronounced for **(B$_1$-**

B_2-B_3)^{SCNP} as compared to **B_1^{SCNP}-B_2-B_3^{SCNP}** (**Figure 5**, **Figure S21, Table 1**) indicating the formation of one SNCP instead of two particles connected by a P(NAM) block as assumed for **B_1^{SCNP}-B_2-B_3^{SCNP}**. This is further supported by the fact that the linear precursor (**B_1-B_2-B_3**) possesses a higher hydrodynamic volume as compared to **B_1^{SCNP}-B_2-B_3**. Additionally, the lower degree of cross linking as determined from ^{1}H-NMR in combination with the decreased hydrodynamic volume of **(B_1-B_2-B_3)^{SCNP}** compared to **B_1^{SCNP}-B_2-B_3^{SCNP}** illustrates the difference between the SCNP obtained by sequential and global folding. All the above results indicate the presence of two distinct folded subdomains within **B_1^{SCNP}-B_2-B_3^{SCNP}** linked by a P(NAM) spacer.

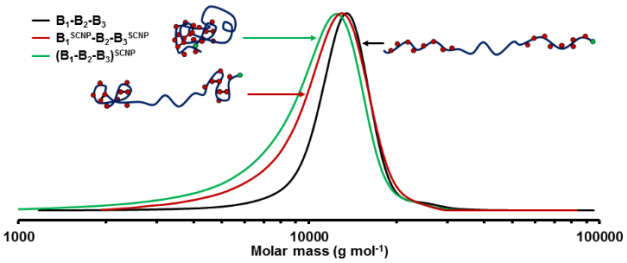

Figure 5. *Overlay of SEC chromatograms (RI traces) obtained in $CHCl_3$ for **B_1^{SCNP}-B_2-B_3^{SCNP}**, **B_1-B_2-B_3** as well as **(B_1-B_2-B_3)^{SCNP}**.*

Synthesis and folding of Penta-block copolymer (B_1^{SCNP}-B_2-B_3^{SCNP}-B_4-B_5^{SCNP})

To explore the potential of the approach, a third chain-extension-folding cycle was attempted. The macro-CTA **B_1^{SCNP}-B_2-B_3^{SCNP}** containing two folded domains was first chain extended with a further spacer block (NAM, **B_4**, DP = 12). Again, a DP of 20 was targeted and 63% of monomer conversion was achieved after 24 h (**Figure S22**). The polymerization was continued after addition of HEA and NAM, to produce the last foldable block with conversions of 85% (NAM) and 84% (HEA), respectively (**B_5**, NAM_{41}-stat-HEA_8, **Figure S23**).

The SEC traces of both chain extensions displayed mono-modal distribution possessing a clear shift to higher molar mass from $\mathbf{B_1^{SCNP}\text{-}B_2\text{-}B_3^{SCNP}}$ to $\mathbf{B_1^{SCNP}\text{-}B_2\text{-}B_3^{SCNP}\text{-}B_4}$ and from $\mathbf{B_1^{SCNP}\text{-}B_2\text{-}B_3^{SCNP}\text{-}B_4}$ to $\mathbf{B_1^{SCNP}\text{-}B_2\text{-}B_3^{SCNP}\text{-}B_4\text{-}B_5}$, respectively (**Figure 6**, **Figure S24**, **Table 1**). The composition of the additional blocks was determined by ^{1}H NMR spectroscopy (**Table 1**, **Figure S25**).

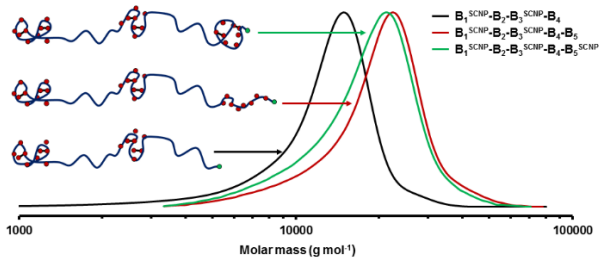

Figure 6. *Overlay of SEC chromatograms (RI traces) obtained in $CHCl_3$ for:* $\boldsymbol{B_1^{SCNP}\text{-}B_2\text{-}B_3^{SCNP}\text{-}B_4}$, $\boldsymbol{B_1^{SCNP}\text{-}B_2\text{-}B_3^{SCNP}\text{-}B_4\text{-}B_5^{SCNP}}$ *and* $\boldsymbol{B_1^{SCNP}\text{-}B_2\text{-}B_3^{SCNP}\text{-}B_4\text{-}B_5}$.

The folding process of the 5th block was carried out using established conditions. After cross linking, the SEC trace in chloroform shows a shift toward lower molar mass species (from 17,500 g mol^{-1} to 16,000 g mol^{-1}, $Đ$ = 1.21, **Figure 6, Figure S26, Table 1**), indicating the formation of a third SCNP. The obtained material was also characterized by ^{1}H NMR spectroscopy (**Figure S25**). Similar to the previous two folding process, the integrals of MDI associated aromatic peaks suggests the addition of two further cross linker molecules. In contrast to previous folding steps, the amount of resulting primary amine functions increased only slightly and more urethane bonds were formed, indicating a higher degree of covalent cross linking for the last block, which could be the result of a lower overall amount of water during cross linking reaction.

Based on the above results, it can also be concluded that this folding process is only within the fifth block $\mathbf{B_5}$. In order to demonstrate this, the penta-block based SCNP ($\mathbf{B_1^{SCNP}\text{-}B_2\text{-}B_3^{SCNP}\text{-}B_4\text{-}B_5^{SCNP}}$) was dissolved in DMF (200 mg mL^{-1}) to break the hydrogen bonds stabilizing the SCNP structure, followed by the dilution with chloroform (to 0.7 mg mL^{-1}). The dilution of DMF with a solvent, which doesn't

interfere with H-Bond formation should lead to the unspecific reformation of cross linking and a change in hydrodynamic volume. This was illustrated by comparing the SEC traces of the initial SCNP (**B_1^{SCNP}-B_2-B_3^{SCNP}-B_4-B_5^{SCNP}**) and the DMF annealed material in $CHCl_3$ (**Figure 7**). The change in elution behaviour shows that the partial interruption of H-bonds by the DMF leads to an increase in compaction after re-cross linking. These results indicate the existence of three individual folded SCNP within the polymer.

Having confirmed the formation of the penta-block based SCNP (**B_1^{SCNP}-B_2-B_3^{SCNP}-B_4-B_5^{SCNP}**) which has three individually cross-linked subdomains, the final material was also characterized by AFM. Diluted chloroform or dichloromethane solutions of **B_1^{SCNP}-B_2-B_3^{SCNP}-B_4-B_5^{SCNP}** at 1 μg mL^{-1} were drop-deposited onto freshly cleaved mica disc. **Figure 8**, **Figure S26** and **Figure S27** showed height map images of the cast surface with a scan size of 1 μm. These figures display that these SCNPs have a height (from the particle peak to the surface of the mica disc) of around 6-8 nm. These size values are relatively high for the described materials,[26, 63] which could indicate aggregation, although similar heights have been reported for AFM profiles of SCNPs.[33] A stiffening of the nanostructure caused by the combination of covalent and supramolecular cross linking could explain the measured height profile of **B_1^{SCNP}-B_2-B_3^{SCNP}-B_4-B_5^{SCNP}** considering size determined by DLS for a single folded subdomain (R_h ≈ 3 nm). However, the feature of three folded subdomains could not be observed in the images. One possible reason might be the insufficient length of the spacer block leading to an aggregation of the single domains after deposition. Furthermore, the complex sample casting process caused by the dewetting effects and evaporative self-assembly[31, 63, 64, 34] resulted the single chain shrink. Nevertheless, the morphology of the SCNPs is expected to be the characteristic sparse "pearl necklace" shape which has been demonstrated by Pomposo and coworkers since the SCNPs were synthesized from the self-avoiding character of the folding blocks in good solvent.[65]

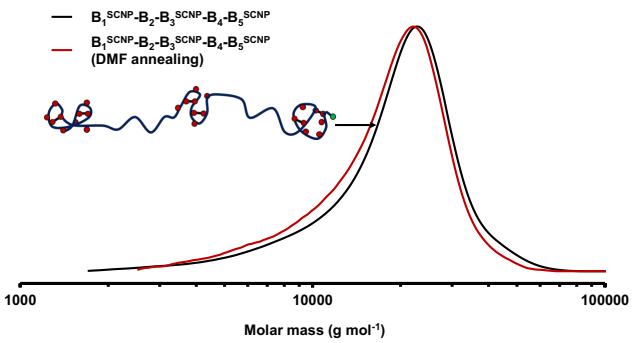

Figure 7. *Overlay of SEC chromatograms (RI traces) obtained in $CHCl_3$ for penta-block based SCNP (B_1^{SCNP}-B_2-B_3^{SCNP}-B_4-B_5^{SCNP}) before and after treatment with DMF sample.*

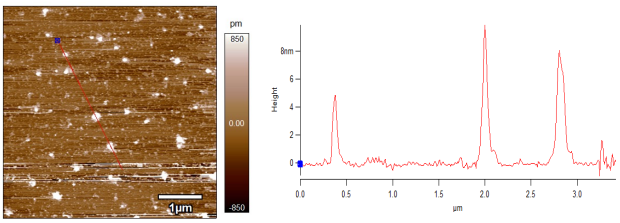

Figure 8. *AFM topography image of penta-block based SCNP B_1^{SCNP}-B_2-B_3^{SCNP}-B_4-B_5^{SCNP} (1 µm × 1 µm scan size, sample dissolved in chloroform).*

CONCLUSION & OUTLOOK

In summary, a complex penta-block containing three individual SCNP segments with an overall dispersity of 1.21 was synthesized using RAFT polymerization. Foldable block consists of a mixture of NAM and HEA, while for polymerization of spacer blocks only NAM was used. The OH groups of HEA were cross linked using a *bis*-isocyanate (MDI) to obtain covalently cross linked SCNP, which in turn also resulted in the formation of urea, as well as amine functions in the cross-linked sections. These moieties were able to further stabilize the SCNP due to hydrogen bonding interactions which were evidenced by ^{1}H-NMR spectroscopy. Control experiments using mono-isocyanates, which are not able to cross link covalently, did solely result in urethane groups, which were not able to form SCNP by supramolecular

interaction. Therefore, it was concluded that described SCNP are stabilized by a synergistic interaction between covalent and supramolecular cross linking.

A chain extension-folding sequence was used to create polymers chains having up to three individual SCNP segments. The cross linking between blocks was ruled out by control experiments using a non-sequential folding procedure. Dissolving the penta-block-tri-SCNP in DMF to interrupt supramolecular connections followed by the dilution in chloroform to reform hydrogen bonds revealed a decreased hydrodynamic volume of DMF annealed sample by SEC analysis in $CHCl_3$ which illustrates the importance of hydrogen bonding, as well as the existence of individual folded domains within the parent penta-block.

The herein presented strategy represents a highly versatile way to produce multi-block SCNP which enables the folding of individual domains within polymer chains. This feature is a further step on the way to copy nature's ability to synthesize highly defined bio-macromolecules with a distinct three dimensional structure. Further work will focus on the introduction of different functionalities enabling orthogonal folding and unfolding within single macromolecules.

ASSOCIATED CONTENT

Supporting Information

Experimental information; ^{1}H-NMR spectra and GPC traces of polymers not depicted in the manuscript.

This material is available free of charge via the Internet at http://pubs.acs.org.

AUTHOR INFORMATION

Corresponding Author

* Correspondence to s.perrier@warwick.ac.uk

ACKNOWLEDGEMENT

The Royal Society Wolfson Merit Award (WM130055; SP), and the Monash-Warwick Alliance is acknowledged for funding (SP; JZ). MH gratefully acknowledges the German Research Foundation (DFG, GZ: HA 7725/1-1) for funding. The authors gratefully acknowledge Oxford Instruments Asylum Research for AFM analysis.

REFERENCES

1. Gody, G.; Maschmeyer, T.; Zetterlund, P. B.; Perrier, S. Rapid and quantitative one-pot synthesis of sequence-controlled polymers by radical polymerization. *Nat. Commun.* **2013,** 4, 2505.
2. Anfinsen, C. B. Principles that Govern the Folding of Protein Chains. *Science* **1973,** 181, (4096), 223-230.
3. Dobson, C. M. Protein folding and misfolding. *Nature* **2003,** 426, (6968), 884-890.
4. Schmidt, B. V.; Fechler, N.; Falkenhagen, J.; Lutz, J. F. Controlled folding of synthetic polymer chains through the formation of positionable covalent bridges. *Nat. Chem.* **2011,** 3, (3), 234-38.
5. Mahon, C. S.; Fulton, D. A. Mimicking nature with synthetic macromolecules capable of recognition. *Nat. Chem.* **2014,** 6, (8), 665-672.
6. ter Huurne, G. M.; Gillissen, M. A. J.; Palmans, A. R. A.; Voets, I. K.; Meijer, E. W. The Coil-to-Globule Transition of Single-Chain Polymeric Nanoparticles with a Chiral Internal Secondary Structure. *Macromolecules* **2015,** 48, (12), 3949-3956.
7. Kirby, A. J. Enzyme Mechanisms, Models, and Mimics. *Angew. Chem. Int. Ed. Engl.* **1996,** 35, (7), 706-724.
8. Liu, Y.; Pauloehrl, T.; Presolski, S. I.; Albertazzi, L.; Palmans, A. R.; Meijer, E. W. Modular Synthetic Platform for the Construction of Functional Single-Chain Polymeric Nanoparticles: From Aqueous Catalysis to Photosensitization. *J. Am. Chem. Soc.* **2015,** 137, (40), 13096-105.
9. Ouchi, M.; Badi, N.; Lutz, J. F.; Sawamoto, M. Single-chain technology using discrete synthetic macromolecules. *Nat. Chem.* **2011,** 3, (12), 917-24.
10. Terashima, T.; Mes, T.; De Greef, T. F. A.; Gillissen, M. A. J.; Besenius, P.; Palmans, A. R. A.; Meijer, E. W. Single-Chain Folding of Polymers for Catalytic Systems in Water. *J. Am. Chem. Soc.* **2011,** 133, (13), 4742-4745.
11. Gillissen, M. A. J.; Voets, I. K.; Meijer, E. W.; Palmans, A. R. A. Single chain polymeric nanoparticles as compartmentalised sensors for metal ions. *Polym. Chem.* **2012,** 3, (11), 3166-3174.
12. Wulff, G.; Chong, B.-O.; Kolb, U. Soluble Single-Molecule Nanogels of Controlled Structure as a Matrix for Efficient Artificial Enzymes. *Angew. Chem. Int. Ed.* **2006,** 45, (18), 2955-2958.

13. Hanlon, A. M.; Lyon, C. K.; Berda, E. B. What Is Next in Single-Chain Nanoparticles? *Macromolecules* **2016,** 49, (1), 2-14.
14. Pomposo, J. A. Bioinspired single-chain polymer nanoparticles. *Polym. Int.* **2014,** 63, (4), 589-592.
15. Altintas, O.; Barner-Kowollik, C. Single-Chain Folding of Synthetic Polymers: A Critical Update. *Macromol. Rapid Commun.* **2016,** 37, (1), 29-46.
16. Lyon, C. K.; Prasher, A.; Hanlon, A. M.; Tuten, B. T.; Tooley, C. A.; Frank, P. G.; Berda, E. B. A brief user's guide to single-chain nanoparticles. *Polym. Chem.* **2015,** 6, (2), 181-197.
17. Mavila, S.; Eivgi, O.; Berkovich, I.; Lemcoff, N. G. Intramolecular Cross-Linking Methodologies for the Synthesis of Polymer Nanoparticles. *Chem. Rev.* **2015**.
18. Altintas, O.; Barner-Kowollik, C. Single chain folding of synthetic polymers by covalent and non-covalent interactions: current status and future perspectives. *Macromol. Rapid Commun.* **2012,** 33, (11), 958-71.
19. Sanchez-Sanchez, A.; Pomposo, J. A. Single-Chain Polymer Nanoparticles via Non-Covalent and Dynamic Covalent Bonds. *Particle & Particle Systems Characterization* **2014,** 31, (1), 11-23.
20. Gonzalez-Burgos, M.; Latorre-Sanchez, A.; Pomposo, J. A. Advances in single chain technology. *Chem. Soc. Rev.* **2015,** 44, (17), 6122-6142.
21. Huo, M.; Wang, N.; Fang, T.; Sun, M.; Wei, Y.; Yuan, J. Single-chain polymer nanoparticles: Mimic the proteins. *Polymer* **2015,** 66, A11-A21.
22. Aiertza, M.; Odriozola, I.; Cabañero, G.; Grande, H.-J.; Loinaz, I. Single-chain polymer nanoparticles. *Cell. Mol. Life Sci.* **2012,** 69, (3), 337-346.
23. Cheng, C.-C.; Chang, F.-C.; Yen, H.-C.; Lee, D.-J.; Chiu, C.-W.; Xin, Z. Supramolecular Assembly Mediates the Formation of Single-Chain Polymeric Nanoparticles. *ACS Macro Letters* **2015,** 4, (10), 1184-1188.
24. Foster, E. J.; Berda, E. B.; Meijer, E. W. Metastable Supramolecular Polymer Nanoparticles via Intramolecular Collapse of Single Polymer Chains. *J. Am. Chem. Soc.* **2009,** 131, (20), 6964-6966.
25. Mes, T.; van der Weegen, R.; Palmans, A. R.; Meijer, E. W. Single-chain polymeric nanoparticles by stepwise folding. *Angew. Chem. Int. Ed. Engl.* **2011,** 50, (22), 5085-9.
26. Berda, E. B.; Foster, E. J.; Meijer, E. W. Toward Controlling Folding in Synthetic Polymers: Fabricating and Characterizing Supramolecular Single-Chain Nanoparticles. *Macromolecules* **2010,** 43, (3), 1430-1437.
27. Hosono, N.; Palmans, A. R. A.; Meijer, E. W. "Soldier-Sergeant-Soldier" triblock copolymers: revealing the folded structure of single-chain polymeric nanoparticles. *Chem. Commun.* **2014,** 50, (59), 7990-7993.
28. Altintas, O.; Krolla-Sidenstein, P.; Gliemann, H.; Barner-Kowollik, C. Single-Chain Folding of Diblock Copolymers Driven by Orthogonal H-Donor and Acceptor Units. *Macromolecules* **2014,** 47, (17), 5877-5888.
29. Altintas, O.; Lejeune, E.; Gerstel, P.; Barner-Kowollik, C. Bioinspired dual self-folding of single polymer chains via reversible hydrogen bonding. *Polym. Chem.* **2012,** 3, (3), 640-651.
30. Stals, P. J. M.; Gillissen, M. A. J.; Paffen, T. F. E.; de Greef, T. F. A.; Lindner, P.; Meijer, E. W.; Palmans, A. R. A.; Voets, I. K. Folding Polymers with Pendant Hydrogen Bonding Motifs in Water: The Effect of Polymer Length and Concentration on the Shape and Size of Single-Chain Polymeric Nanoparticles. *Macromolecules* **2014,** 47, (9), 2947-2954.
31. van Roekel, H. W. H.; Stals, P. J. M.; Gillissen, M. A. J.; Hilbers, P. A. J.; Markvoort, A. J.; de Greef, T. F. A. Evaporative self-assembly of single-chain, polymeric nanoparticles. *Chem. Commun.* **2013,** 49, (30), 3122-3124.
32. Beck, J. B.; Killops, K. L.; Kang, T.; Sivanandan, K.; Bayles, A.; Mackay, M. E.; Wooley, K. L.; Hawker, C. J. Facile Preparation of Nanoparticles by Intramolecular Crosslinking of Isocyanate Functionalized Copolymers. *Macromolecules* **2009,** 42, (15), 5629-5635.
33. Hansell, C. F.; Lu, A.; Patterson, J. P.; O'Reilly, R. K. Exploiting the tetrazine-norbornene reaction for single polymer chain collapse. *Nanoscale* **2014,** 6, (8), 4102-7.

34. Wong, E. H. H.; Lam, S. J.; Nam, E.; Qiao, G. G. Biocompatible Single-Chain Polymeric Nanoparticles via Organo-Catalyzed Ring-Opening Polymerization. *ACS Macro Letters* **2014,** 3, (6), 524-528.
35. Beck, J. B.; Killops, K. L.; Kang, T.; Sivanandan, K.; Bayles, A.; Mackay, M. E.; Wooley, K. L.; Hawker, C. J. Facile Preparation of Nanoparticles by Intramolecular Cross-Linking of Isocyanate Functionalized Copolymers. *Macromolecules* **2009,** 42, (15), 5629-5635.
36. Sugai, N.; Heguri, H.; Yamamoto, T.; Tezuka, Y. A Programmed Polymer Folding: Click and Clip Construction of Doubly Fused Tricyclic and Triply Fused Tetracyclic Polymer Topologies. *J. Am. Chem. Soc.* **2011,** 133, (49), 19694-19697.
37. Song, C.; Li, L.; Dai, L.; Thayumanavan, S. Responsive single-chain polymer nanoparticles with host–guest features. *Polym. Chem.* **2015,** 6, (26), 4828-4834.
38. Sanchez-Sanchez, A.; Fulton, D. A.; Pomposo, J. A. pH-responsive single-chain polymer nanoparticles utilising dynamic covalent enamine bonds. *Chem. Commun.* **2014,** 50, (15), 1871-1874.
39. Whitaker, D. E.; Mahon, C. S.; Fulton, D. A. Thermoresponsive Dynamic Covalent Single-Chain Polymer Nanoparticles Reversibly Transform into a Hydrogel. *Angew. Chem. Int. Ed.* **2013,** 52, (3), 956-959.
40. Shishkan, O.; Zamfir, M.; Gauthier, M. A.; Borner, H. G.; Lutz, J.-F. Complex single-chain polymer topologies locked by positionable twin disulfide cyclic bridges. *Chem. Commun.* **2014,** 50, (13), 1570-1572.
41. Badi, N.; Lutz, J. F. Sequence control in polymer synthesis. *Chem. Soc. Rev.* **2009,** 38, (12), 3383-90.
42. Lutz, J.-F. Sequence-controlled polymerizations: the next Holy Grail in polymer science? *Polym. Chem.* **2010,** 1, (1), 55.
43. Lutz, J.-F.; Ouchi, M.; Liu, D. R.; Sawamoto, M. Sequence-Controlled Polymers. *Science* **2013,** 341, (6146).
44. Gody, G.; Maschmeyer, T.; Zetterlund, P. B.; Perrier, S. Exploitation of the Degenerative Transfer Mechanism in RAFT Polymerization for Synthesis of Polymer of High Livingness at Full Monomer Conversion. *Macromolecules* **2014,** 47, (2), 639-649.
45. Gody, G.; Maschmeyer, T.; Zetterlund, P. B.; Perrier, S. Pushing the Limit of the RAFT Process: Multiblock Copolymers by One-Pot Rapid Multiple Chain Extensions at Full Monomer Conversion. *Macromolecules* **2014,** 47, (10), 3451-3460.
46. Lutz, J.-F. Polymer chemistry: A controlled sequence of events. *Nat. Chem.* **2010,** 2, (2), 84-85.
47. Roy, R. K.; Lutz, J. F. Compartmentalization of single polymer chains by stepwise intramolecular cross-linking of sequence-controlled macromolecules. *J. Am. Chem. Soc.* **2014,** 136, (37), 12888-91.
48. Harth, E.; Horn, B. V.; Lee, V. Y.; Germack, D. S.; Gonzales, C. P.; Miller, R. D.; Hawker, C. J. A Facile Approach to Architecturally Defined Nanoparticles via Intramolecular Chain Collapse. *J. Am. Chem. Soc.* **2002,** 124, (29), 8653-8660.
49. Gody, G.; Rossner, C.; Moraes, J.; Vana, P.; Maschmeyer, T.; Perrier, S. One-Pot RAFT/"Click" Chemistry via Isocyanates: Efficient Synthesis of α-End-Functionalized Polymers. *J. Am. Chem. Soc.* **2012,** 134, (30), 12596-12603.
50. Coca, S.; Jasieczek, C. B.; Beers, K. L.; Matyjaszewski, K. Polymerization of acrylates by atom transfer radical polymerization. Homopolymerization of 2-hydroxyethyl acrylate. *J. Polym. Sci., Part A: Polym. Chem.* **1998,** 36, (9), 1417-1424.
51. Ferguson, C. J.; Hughes, R. J.; Nguyen, D.; Pham, B. T. T.; Gilbert, R. G.; Serelis, A. K.; Such, C. H.; Hawkett, B. S. Ab Initio Emulsion Polymerization by RAFT-Controlled Self-Assembly§. *Macromolecules* **2005,** 38, (6), 2191-2204.
52. Pomposo, J. A.; Perez-Baena, I.; Buruaga, L.; Alegría, A.; Moreno, A. J.; Colmenero, J. On the Apparent SEC Molecular Weight and Polydispersity Reduction upon Intramolecular Collapse of Polydisperse Chains to Unimolecular Nanoparticles. *Macromolecules* **2011,** 44, (21), 8644-8649.

53. Tuten, B. T.; Chao, D.; Lyon, C. K.; Berda, E. B. Single-chain polymer nanoparticles via reversible disulfide bridges. *Polym. Chem.* **2012,** 3, (11), 3068-3071.
54. Murray, B. S.; Fulton, D. A. Dynamic Covalent Single-Chain Polymer Nanoparticles. *Macromolecules* **2011,** 44, (18), 7242-7252.
55. Buurma, N. J.; Cook, J. L.; Hunter, C. A.; Low, C. M. R.; Vinter, J. G. The role of functional group concentration in solvation thermodynamics. *Chemical Science* **2010,** 1, (2), 242-246.
56. Catrouillet, S.; Fonteneau, C.; Bouteiller, L.; Delorme, N.; Nicol, E.; Nicolai, T.; Pensec, S.; Colombani, O. Competition Between Steric Hindrance and Hydrogen Bonding in the Formation of Supramolecular Bottle Brush Polymers. *Macromolecules* **2013,** 46, (19), 7911-7919.
57. Liu, J. W.; Mackay, M. E.; Duxbury, P. M. Molecular Dynamics Simulation of Intramolecular Cross-Linking of BCB/Styrene Copolymers. *Macromolecules* **2009,** 42, (21), 8534-8542.
58. Higashijima, T.; Tasumi, M.; Miyazawa, T. 1H Nuclear magnetic resonance studies of melanostatin: Dependence of the chemical shifts of NH protons on temperature and concentration. *FEBS Letters* **1975,** 57, (2), 175-178.
59. Boileau, S.; Bouteiller, L.; Laupretre, F.; Lortie, F. Soluble supramolecular polymers based on urea compounds. *New Journal of Chemistry* **2000,** 24, (11), 845-848.
60. Mecerreyes, D.; Lee, V.; Hawker, C. J.; Hedrick, J. L.; Wursch, A.; Volksen, W.; Magbitang, T.; Huang, E.; Miller, R. D. A Novel Approach to Functionalized Nanoparticles: Self-Crosslinking of Macromolecules in Ultradilute Solution. *Adv. Mater.* **2001,** 13, (3), 204-208.
61. Cherian, A. E.; Sun, F. C.; Sheiko, S. S.; Coates, G. W. Formation of Nanoparticles by Intramolecular Cross-Linking: Following the Reaction Progress of Single Polymer Chains by Atomic Force Microscopy. *J. Am. Chem. Soc.* **2007,** 129, (37), 11350-11351.
62. Zhong, M.; Matyjaszewski, K. How Fast Can a CRP Be Conducted with Preserved Chain End Functionality? *Macromolecules* **2011,** 44, (8), 2668-2677.
63. Altintas, O.; Willenbacher, J.; Wuest, K. N. R.; Oehlenschlaeger, K. K.; Krolla-Sidenstein, P.; Gliemann, H.; Barner-Kowollik, C. A Mild and Efficient Approach to Functional Single-Chain Polymeric Nanoparticles via Photoinduced Diels–Alder Ligation. *Macromolecules* **2013,** 46, (20), 8092-8101.
64. Rabani, E.; Reichman, D. R.; Geissler, P. L.; Brus, L. E. Drying-mediated self-assembly of nanoparticles. *Nature* **2003,** 426, (6964), 271-274.
65. Pomposo, J. A.; Perez-Baena, I.; Lo Verso, F.; Moreno, A. J.; Arbe, A.; Colmenero, J. How Far Are Single-Chain Polymer Nanoparticles in Solution from the Globular State? *ACS Macro Letters* **2014,** 3, (8), 767-772.

SYNOPSIS TOC